

1 Integrating Earth Observation and Ecological Modeling to 2 Advance Sustainability Assessment of Cocoa Expansion

3 Shuntian Wang^{1,2*}, Yue Yu^{1,*}, Christie Walker¹, Jorge Perez³, Wendy Francesconi³, Jhon Tello³,
4 Louis Reymondin³, Stephan Pfister^{1,2}

5 ¹*Ecological Systems Design, Institute of Environmental Engineering, ETH Zurich*

6 ²*Institute of Science, Technology and Policy, ETH Zurich*

7 ³*Alliance of Bioversity International and CIAT*

8 *Contact of corresponding author: shuntian.wang@ifu.baug.ethz.ch, yueyuy@ethz.ch

9 ***SI Table of Contents***

10 **Supplementary Text**

11 **Text S1.** Region of interest: Ucayali Agroecological Living Landscape (UALL), Peru

12 **Text S2.** Quantification of the loss of water purification services from cocoa-driven deforestation

13 **Supplementary Figures**

14 **Figure S1.** Location map of the Agroecological Living Landscape (UALL).

15 **Figure S2.** The workflow for mapping LULC by leveraging multi-source satellite imagery and machine learning
16 for classification.

17 **Supplementary Tables**

18 **Table S1.** Assigned mean species abundance (MSA) values for animals and plants corresponding to different
19 LULC classes used as input parameters in the GLOBIO4 model.

20 **Table S2.** The identification of nature land cover and human land use based on the LULC code.

21 **Table S3.** LULC-Specific Biophysical Parameters for NDR Modeling.

22 **Table S4.** The area of direct deforestation caused by cocoa cultivation in each district of UALL (measured in
23 hectares).

24 **Table S5.** The area and rate of deforestation from 2000 to 2020 in each district (measured in hectares).

25 **References**

26 **Text S1. Region of interest: Ucayali Agroecological Living Landscape (UALL), Peru**

27 The Ucayali department lies in the central-eastern Peruvian Amazon, encompassing four
28 provinces—Coronel Portillo, Padre Abad, Atalaya, and Purús—and spanning 102,400 km².
29 Within this region, the Agroecological Living Landscape (UALL) for the CGIAR Agroecology
30 Initiative includes the entirety of Padre Abad Province, along with the districts of Nueva
31 Requena, Campoverde, Manantay, and Yarinacocha in Coronel Portillo Province (home to the
32 regional capital, Pucallpa). Spanning 14,064 km², roughly 14% of Ucayali's total area, the UALL
33 closely aligns with the regionally designated Agroecological Corridor, known as the Cuenca de
34 Aguaytía (Pareja et al., 2023).

35 Ucayali features a warm-humid climate characteristic of the Amazonian bioclimatic region,
36 with a departmental multi-year mean temperature of ~26 °C and rainfall of ~2,000 mm per
37 year (2000–2015 baseline) (Castro et al., 2021; Pareja et al., 2023). The UALL encompasses
38 two distinct sub-zones: a cooler, wetter sub-Andean western sector (min ~10 °C; max ~31 °C;
39 3,000–4,500 mm precipitation per year) and a drier, warmer Amazon plain that hosts the
40 majority of agricultural activity (min ~19 °C; max ~32 °C; 1,200–3,000 mm precipitation per
41 year). Predominantly shaped by the Aguaytía River basin—a major tributary of the Ucayali
42 River—the UALL saw licensed consumptive water use in 2021 heavily dominated by
43 agriculture (~94% of the granted volume), followed by domestic, industrial, and other uses.

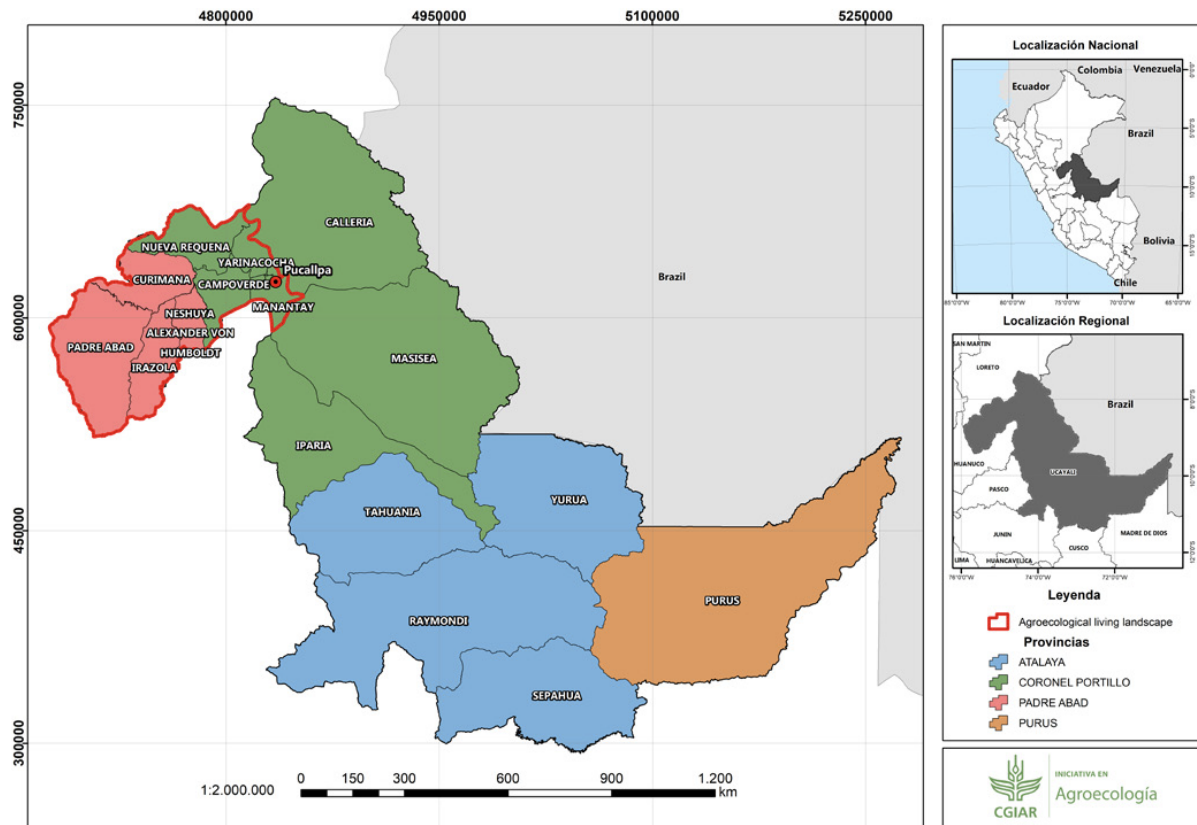
44 The physiographic diversity of the UALL is striking, encompassing three major provinces: the
45 Andean Mountain Range (sub-Andean zone), the Amazon sedimentary basin (Amazon plain),
46 and the Sierra del Divisor. This mosaic results in a landscape dominated by mountains (~15%),
47 hills (~40%), and plains/terraces (~43%), transitioning from rugged sub-Andean terrain in the
48 Aguaytía headwaters to expansive alluvial lowlands at its confluence with the Ucayali River
49 (Pareja et al., 2023). Land-use capacity assessments, grounded in Ecological Economic Zoning,
50 reveal that 58% of the UALL is ideally suited for protection or sustainable forest production.
51 Merely 33% is deemed appropriate for agricultural pursuits (albeit with notable limitations),
52 while the remaining ~9% consists of zones with mixed agricultural potential embedded within
53 protective forest areas.

54 Ucayali holds national significance for biodiversity conservation, containing approximately
55 9.21 million hectares of forests (“Resolución Ministerial N.º 179-2021-MINAM,” n.d.) and 10
56 Protected Natural Areas (PNAs) that total ~2.26 million hectares, covering ~22% of the
57 departmental area. The UALL itself includes four PNAs: Cordillera Azul National Park (~73,901
58 hectares) and three private conservation areas (~5,320 hectares total). Regional inventories
59 document remarkable species richness, including ~1,600 plant species, >377 fish, 402
60 amphibians, 82 reptiles, 782 birds, and 257 mammals (J, 2022; Pareja et al., 2023). The
61 dominant Selva Baja ecozone is characterized by high tree density (~458 individuals per
62 hectare; DBH ≥10 cm) and contains the highest estimated carbon stock among all Peruvian
63 ecozones, at ~138.84 Mg C per hectare (Silvestre, 2020).

64 Ucayali has experienced substantial historical forest loss, totaling ~1.03 million hectares, with
65 approximately half of this loss occurring between 2001 and 2021. This deforestation is
66 disproportionately concentrated within the UALL, which accounted for ~55% of the
67 department's total forest loss during this period. By 2021, roughly 40% of the UALL's original

68 forest cover had been cleared (Pareja et al., 2023; “Resolución Ministerial N.º 179-2021-
69 MINAM,” n.d.) The principal proximate drivers are agricultural expansion—for crops such as
70 oil palm, cocoa, and pasture—and infrastructure development, particularly roads. These
71 pressures are compounded by underlying factors including limited governance capacity, weak
72 regulatory enforcement, poor inter-sectoral coordination, and corruption, all of which elevate
73 forest conversion risk.

74 Ucayali is a key national producer of cocoa, ranking third in output with ~21,600 tons
75 harvested in 2021 (Charry et al., 2023). Production has surged in the past decades, driven
76 primarily by area expansion rather than yield intensification (mean ~977 kg per hectare in
77 2021). This production is highly concentrated in the UALL, which accounts for ~72% of
78 departmental production and ~76% of the harvested area. Cocoa cultivation is dominated by
79 small- to medium-scale farmers, with a mean agricultural unit size of ~23 hectares, of which
80 ~2 hectares is dedicated to cocoa (Pareja et al., 2023). These farms are typically diversified,
81 commonly integrating banana (~62%), cassava (~25%), and other subsistence and cash crops,
82 alongside small-scale livestock. The field design for cocoa plantations typically employs a 3×3
83 m spacing (in square or triangular arrangements), corresponding to a density of approximately
84 1,100–1,300 plants per hectare (Goñas et al., 2022; Rojas-Briceño et al., 2022). For clones with
85 low to medium vigor where higher densities are desired, a 3×2 m configuration (≈1,666
86 plants/ha) is also common. Shade cover is maintained at 30–50% during the first two years of
87 plantation establishment and is gradually reduced to approximately 20% (typically 10–20%)
88 as the cocoa canopy closes to ensure adequate ventilation and light penetration (Rajab et al.,
89 2016). Pruning management begins with formation pruning after planting to define the trunk
90 and select 3–4 primary branches ((Goñas et al., 2022; Rojas-Briceño et al., 2022)). This is
91 followed by maintenance pruning approximately every 6 months to remove chupons (water
92 sprouts), crossing, diseased, or dead branches, and basal suckers, with phytosanitary pruning
93 performed as needed. During the productive phase, tree height is controlled at around 3–4 m
94 to facilitate harvesting and mitigate disease risk (Goñas et al., 2022; Rojas-Briceño et al., 2022).
95 This approach helps maintain robust yields and ecosystem services in a complex landscape
96 where conventional and organic systems operate alongside high-carbon forests and sensitive
97 hydrological systems. Market segmentation exists between conventional and certified organic
98 producers, with the latter estimated to represent ~38% of the cocoa area (2020) (Pareja et al.,
99 2023). The UALL thus represents a critical tropical agricultural landscape, where the expansion
100 of smallholder cocoa mosaics directly interfaces with high-carbon, biodiversity-rich forests
101 and water quality sensitive systems.



102
 103 **Figure S1.** Location map of the Agroecological Living Landscape (UALL). The map displays the geographical
 104 location of the UALL within Peru, highlighting its position in the Ucayali region and showing the specific
 105 administrative districts included. Two inset maps provide context: the upper inset shows the location of the
 106 Ucayali region within Peru, while the lower inset details the regional boundaries. This map was directly
 107 referenced from "Analysis of the context and agroecological principles in Ucayali's ALL" by Piedad Pareja.

108
 109 **Text S2. Quantification of the loss of water purification services from cocoa-driven**
 110 **deforestation**

111 To quantify the degradation of the water purification service, this study simulated the increase
 112 in nitrogen (N) export resulting from cocoa-driven deforestation. The assessment was
 113 conducted using the Nutrient Delivery Ratio (NDR) model, a component of the Integrated
 114 Valuation of Ecosystem Services and Tradeoffs (InVEST) software suite developed by the
 115 Natural Capital Project (Natural Capital Project, 2024). The NDR model is specifically designed
 116 to map nutrient sources from watersheds and their transport to stream networks, providing
 117 a spatially explicit quantification of nutrient retention by natural vegetation. By simulating
 118 how LULC change affects nutrient runoff from non-point terrestrial sources, the model
 119 provides a powerful tool for assessing impacts on water quality. The primary objective of its
 120 application in this study was to quantify the change in nitrogen retention capacity of the
 121 landscape following the conversion of native forest to cocoa cultivation.

122 The InVEST NDR model is a spatially explicit, empirical model that estimates the long-term,
 123 steady-state export of nutrients from each pixel on a landscape to the adjacent stream
 124 network. Unlike more sophisticated, process-based biogeochemical models that require
 125 extensive and often unavailable input data, the NDR model leverages simplified empirical

126 relationships to simulate nutrient cycling and transport. This approach makes it exceptionally
127 well-suited for regional-scale assessments in data-limited contexts, such as the agricultural
128 landscapes of the Amazon basin. The model's logic is centered on two fundamental processes
129 that are calculated for each grid cell in the landscape: (1) Nutrient Loading: This represents
130 the gross amount of a nutrient generated on a given grid cell, which is primarily a function of
131 its LULC type and local runoff potential. (2) Nutrient Delivery: This represents the proportion
132 of the nutrient load from a pixel that is transported downslope and ultimately reaches the
133 stream. This proportion is determined by the hydrological connectivity of the pixel to the
134 stream and the nutrient retention capacity of the downslope flow path.

135 The total nutrient export from a pixel is calculated as the product of its nutrient load and its
136 NDR. The model accounts for two primary nutrient transport pathways: surface runoff and
137 subsurface flow. This distinction is particularly important for nitrogen, a portion of which is
138 highly mobile as dissolved nitrate in groundwater. The model partitions the total load on a
139 pixel into surface and subsurface components based on a user-defined parameter,
140 `proportion_subsurface_n`, which quantifies the ratio of dissolved nutrients to the total
141 nutrient amount. The NDR for a pixel is a critical component that reflects its position in the
142 landscape and the filtering capacity of downslope ecosystems. It is calculated as a function of
143 several factors, most notably the Index of Connectivity (IC) and the retention efficiency of
144 LULC types along the flow path. The IC is a topographic index derived from the Digital Elevation
145 Model (DEM) that represents the hydrological connectivity, or the likelihood that a nutrient
146 on a pixel will reach the stream. The model calculates the proportion of nutrients that are not
147 retained by downslope pixels, considering their LULC-specific retention efficiencies and a
148 characteristic retention length. The final NDR value integrates these factors to estimate what
149 fraction of the nutrient load from the pixel will be delivered to the stream.

150 The selection of the InVEST NDR model for this analysis was a strategic decision that balanced
151 the need for quantitative, spatially explicit outputs with the practical constraints of data
152 availability in the study region. The UALL is a dynamic agricultural landscape, a context often
153 characterized by a scarcity of the detailed, long-term data required by more complex
154 hydrological models (e.g., SWAT). Such models typically demand extensive parameterization,
155 including detailed soil physics, daily meteorological data, and precise fertilizer and manure
156 application rates, which are not available at the scale of this analysis. The InVEST NDR model
157 is designed precisely for these conditions. It provides robust, quantitative estimates of
158 nutrient export in physical units (kg/year), which is essential for assessing ecosystem service
159 loss, without imposing prohibitive data requirements. The model's primary strength, and a
160 key reason for its selection, lies in its application for scenario comparison. By running the
161 model for a baseline (pre-deforestation) scenario and a current (post-deforestation) scenario
162 while holding all other inputs constant, the analysis can robustly quantify the change in
163 nutrient export attributable solely to LULC change.

164 The NDR model requires a suite of geospatial data layers to simulate nutrient transport across
165 the landscape. Each dataset was carefully selected and pre-processed to ensure consistency
166 in spatial resolution, projection, and extent, thereby guaranteeing the analytical integrity of
167 the model runs.

168 A high-quality Digital Elevation Model (DEM) is the foundational dataset for the NDR model,
169 as it is used to derive all topographic and hydrological characteristics of the landscape. The
170 analysis utilized the Shuttle Radar Topography Mission (SRTM) 1 Arc-Second Global digital
171 elevation model. Specifically, the void-filled Version 3 product (SRTMGL1 v003), provided by
172 the NASA Jet Propulsion Laboratory (JPL) (NASA Jet Propulsion Laboratory and NASA, 2013),
173 was selected. This dataset has a spatial resolution of approximately 30 m at the equator and
174 was generated from data collected by the Space Shuttle Endeavour in February 2000. Data
175 tiles covering the study region were acquired through the U.S. Geological Survey (USGS)
176 EarthExplorer portal. Individual SRTM tiles were mosaicked to create a single, continuous
177 elevation raster covering the entire UALL study area. The mosaicked DEM was then projected
178 to the appropriate Universal Transverse Mercator (UTM) zone for the central Peruvian
179 Amazon to ensure that all distance and area calculations performed by the model were
180 accurate. No manual hydrological conditioning (e.g., sink filling or stream burning) was
181 performed on the DEM, as the InVEST software suite includes robust internal algorithms to
182 pre-process the elevation data and derive hydrologically consistent flow paths. The DEM is
183 used by the model to compute flow direction, flow accumulation, slope gradients, and the
184 critical Index of connectivity that governs the simulated pathways of nutrient transport from
185 land to water.

186 The LULC maps serve as the primary drivers of spatial heterogeneity in the model, defining
187 both the location and magnitude of nutrient sources and retention sinks across the landscape.
188 To specifically isolate the impact of cocoa-driven deforestation, two distinct LULC maps were
189 prepared. The Baseline scenario represents a hypothetical landscape in 2020 without cocoa-
190 driven deforestation, where pixels classified as cocoa in 2020 were reassigned to their original
191 forest or other pre-cocoa land cover from the year 2000. The Current Scenario represents the
192 actual contemporary landscape of 2020, explicitly reflecting cocoa-driven deforestation that
193 occurred between 2000 and 2020. Both LULC maps were prepared as raster datasets with the
194 same spatial resolution (~10 m), coordinate projection (UTM), and DEM to ensure precise cell-
195 by-cell alignment. Integer codes (lucode) assigned to each land cover class in these rasters
196 were matched with corresponding codes in the biophysical input table (see Table S3). The
197 LULC map thus acts as the core variable in this analysis, as the model relies on the lucode of
198 each grid cell to assign its nitrogen load and retention efficiency parameters. Given that the
199 LULC map was the only parameter altered between these two model simulations, any
200 differences in nitrogen export can be directly attributed to cocoa-driven deforestation.

201 A spatially explicit proxy for runoff potential is required by the model to weight nutrient
202 generation across the landscape. Mean annual precipitation was used as the runoff proxy.
203 Data were from the PISCOp (Peruvian Interpolated data of the SENAMHI's Climatological and
204 hydrological Observations) V2.1 dataset (Aybar et al., 2019). PISCOp is a high-resolution
205 gridded precipitation product developed specifically for Peru. It is generated by blending
206 quality-controlled in-situ rain gauge data from the extensive network of the Peruvian National
207 Meteorology and Hydrology Service with satellite-based precipitation estimates. This blending
208 process results in a robust, locally calibrated product that is highly valuable for hydrological
209 applications in Peru. The dataset has a native resolution of 0.1 degrees (approximately 10 km)
210 and provides data from 1981 to the present. To create a long-term average, monthly PISCOp

211 data for the period 2000–2020 were aggregated to calculate a mean annual precipitation
212 raster. This coarse-resolution raster was then resampled to the 10 m resolution of the LULC
213 using a bilinear interpolation method. This step produced a smooth, continuous surface of
214 precipitation values that reflects regional climate patterns. In the model, this raster acts as a
215 weighting factor; areas with higher mean annual precipitation are assumed to have greater
216 surface runoff, leading to a higher potential for nutrient mobilization and transport. The
217 decision to use the PISCOp dataset instead of a more readily available global precipitation
218 product (e.g., GPCP) significantly enhances the regional accuracy of this analysis. The study
219 area spans a sharp environmental gradient, which creates complex orographic effects and
220 steep precipitation gradients. Coarse-resolution global datasets often fail to capture this fine-
221 scale variability. Because PISCOp is specifically calibrated for Peru and incorporates thousands
222 of local rain gauge observations, it provides a much more realistic representation of these
223 precipitation patterns. This commitment to using the best available, locally-validated data
224 improves the reliability of the runoff proxy and, by extension, the entire nutrient export
225 simulation.

226 Watershed boundaries were defined using the HydroBASINS dataset (Lehner, 2014).
227 HydroBASINS provides a globally consistent, multi-level suite of hierarchically nested
228 watershed polygons, which is itself based on SRTM DEM data. The dataset employs the
229 Pfafstetter coding system, a topological scheme that allows for the delineation of nested sub-
230 basins from continental scale (Level 1) to very fine scales (Level 12). For this regional-scale
231 analysis, Pfafstetter Level 9 basins were selected as the aggregation unit. The global
232 HydroBASINS shapefile for South America was obtained and clipped to the spatial extent of
233 the study area.

234 Threshold flow accumulation defines the minimum number of upslope pixels that must drain
235 into a given pixel for it to be classified as part of a stream network. It is derived directly from
236 the DEM and strongly influences the delineation of hydrologic connectivity and subsequent
237 nutrient export estimates. When a flow path intersects a stream, nutrient retention processes
238 cease, and any nutrients reaching the stream channel are assumed to be exported to the
239 catchment outlet. Therefore, selecting an appropriate threshold is critical to ensure that
240 modeled stream networks closely match actual stream conditions. After extensive validation
241 against observed stream data, we chose a threshold value of 3000.

242 The biophysical table is a critical input that parameterizes the model by linking each LULC class
243 to its associated nutrient loading and retention characteristics. The parameters used in this
244 study were compiled based on a review of relevant literature for tropical agriculture and
245 forestry systems, and are presented in Table S3. This table provides the core assumptions
246 driving the model's simulation of nutrient dynamics.

247 Nitrogen Load (load_n): This parameter represents the gross amount of nitrogen generated
248 on-site per hectare per year for each LULC class, before accounting for landscape retention.
249 The parameterization of load_n directly encodes the central hypothesis of the study. The value
250 for intact forest is set at a low baseline of 0.9 kg/hectare/year, representing background
251 nitrogen cycling in a natural ecosystem. In stark contrast, the values for intensive agricultural
252 systems like Cocoa (15.0 kg/hectare/year) and Oil Palm (25.0 kg/hectare/year) are orders of

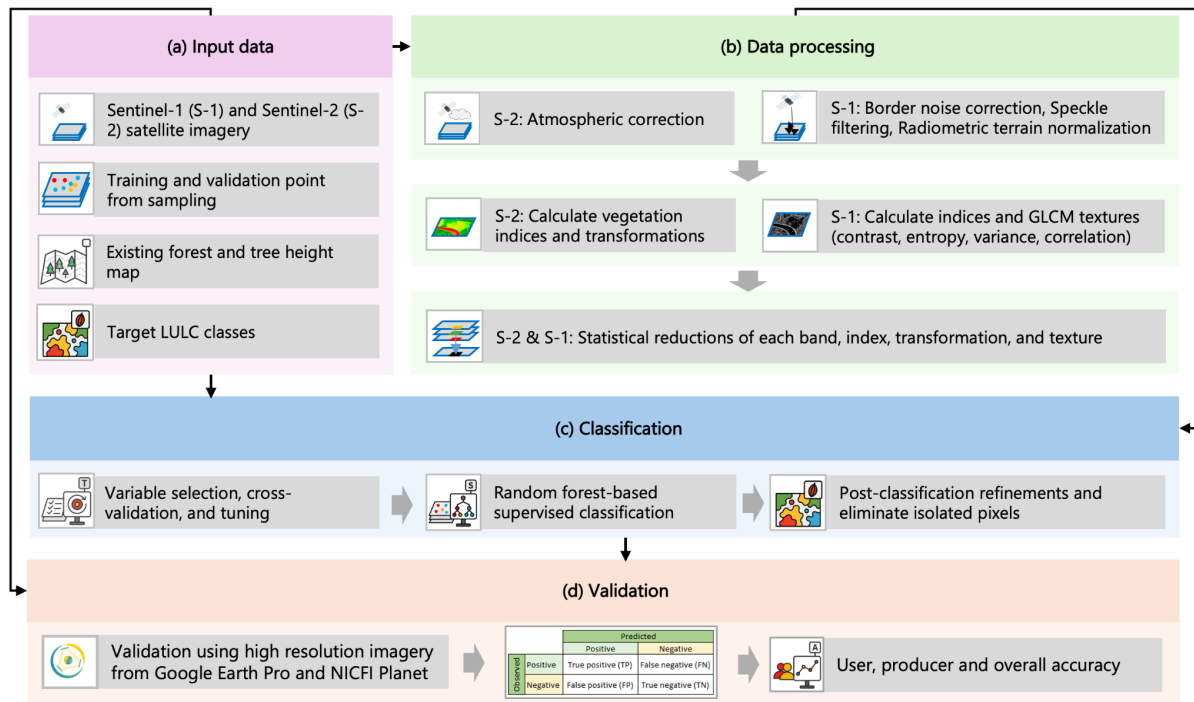
253 magnitude higher. These elevated values reflect external nutrient inputs from synthetic
254 fertilizers, the rapid mineralization of soil organic matter following land clearing, and
255 increased soil erosion. This differential ensures that the model simulates a substantial increase
256 in nitrogen loading on any pixel converted from forest to agriculture.

257 Nitrogen Retention Efficiency (*eff_n*): This parameter defines the proportion of nutrients that
258 are retained, removed, or uptaken as they flow over a pixel of a given LULC type. It quantifies
259 the landscape's natural filtration capacity. The values assigned to this parameter represent
260 the secondary impact of deforestation: the degradation of the landscape's ability to regulate
261 nutrient flows. Forest is assigned a very high retention efficiency (0.80), reflecting the capacity
262 of its dense multi-layered canopy, complex root systems, and thick organic soil horizons to
263 trap and assimilate nutrients. Conversely, agricultural lands (e.g., Cocoa at 0.60, Pastures at
264 0.35) and especially Urban areas (0.05) are assigned much lower efficiencies. This reflects their
265 simplified vegetation structure, compacted soils, and more impervious surfaces, which
266 facilitate rapid runoff rather than filtration. Therefore, deforestation not only increases the
267 source of nitrogen pollution but also simultaneously reduces the landscape's inherent ability
268 to mitigate its transport to waterways.

269 Proportion of Subsurface Flow (*proportion_subsurface_n*): This parameter determines the
270 fraction of the total nitrogen load that is transported via subsurface pathways as dissolved
271 nutrients. Forest is assigned a high value (0.60), reflecting the high infiltration rates and soil
272 porosity characteristic of undisturbed forest soils. Agricultural and urban lands, which often
273 have more compacted soils and higher rates of surface runoff, are assigned lower values.

274 Retention Length (*crit_len_n*): This parameter defines the distance (in meters) over which a
275 given LULC type is assumed to reach its maximum retention efficiency. In the absence of
276 specific empirical data for the diverse LULC types in the study region, this parameter was held
277 constant at 200 meters for all classes. This is a common and practical approach in regional-
278 scale InVEST applications and ensures that the relative differences in retention capacity
279 between LULC types are driven by the more sensitive *eff_n* parameter. Other parameters in
280 the model use InVEST NDR's default settings.

281 We quantified the degradation of water purification services as the net change in annual
282 nitrogen export between the two scenarios. On the resulting map, positive values indicate
283 degradation of this service. The resulting metric enables the direct identification and ranking
284 of regions with the greatest service degradation. This approach explicitly links landscape-scale
285 deforestation patterns to their cumulative downstream hydrological consequences.
286 Ultimately, the aggregated map serves as a decision-support tool for prioritizing conservation,
287 restoration, and management efforts in watersheds most impacted by agricultural expansion.



288

289 **Figure S2:** The workflow for mapping LULC by leveraging multi-source satellite imagery and machine learning for
 290 classification. (a) Input data: Acquisition of Sentinel-1 radar and Sentinel-2 optical satellite imagery,
 291 supplemented by training and validation points, an existing forest map, and tree height data, as well as the
 292 definitions of 10 target land cover classes. (b) Data processing: Atmospheric correction applied to Sentinel-2 data,
 293 followed by calculation of vegetation indices, transformations, and statistics; for Sentinel-1 data, border noise
 294 removal, speckle filtering, and radiometric terrain normalization; derivation of GLCM textures (contrast, entropy,
 295 variance, correlation) with a small window, with statistical reductions (mean, median, standard deviation,
 296 maximum, minimum) to create normalized multiband compositions. (c) Classification: Training and validation,
 297 followed by feature selection, cross-validation, hyperparameter tuning, and supervised classification with a
 298 random forest algorithm; post-classification refinements include application of overlapping masks and a majority
 299 filter to eliminate isolated pixels and mitigate noise. (d) Validation results: Accuracy assessment using high-
 300 resolution imagery from Google Earth Pro and NICFI Planet, incorporating a confusion matrix to compute user
 301 accuracy, producer accuracy, and overall accuracy, under a stratified random sampling design. Arrows indicate
 302 sequential data processing flows between stages.

303 **Table S1.** Assigned mean species abundance (MSA) values for animals and plants corresponding to different LULC
 304 classes used as input parameters in the GLOBIO4 model.

LULC code	LULC description	MSA vertebrates	MSA plants
1	Agriculture	0.452	0.156
2	Urban	0.264	0.361
3	Bare soil	1	1
4	Forest	1	1
5	Water	0	0
6	Pasture	0.401	0.149
7	Secondary vegetation	0.621	0.568
8	Oil palm	0.452	0.156
9	Other plantations	0.621	0.568
10	Cocoa	0.452	0.156

305

306 **Table S2.** The identification of nature land cover and human land use based on the LULC code.

LULC description	GLOBIO 4 Category
Nature land cover	Forest, Secondary vegetation, Bare soil
Human land use	Agriculture, Urban, Pasture, Oil palm, Other plantations, Cocoa

307

308 **Table S3.** LULC-Specific Biophysical Parameters for NDR Modeling

lucode	LULC Description	Nitrogen Load (kg/ha/yr)	Nitrogen Retention Efficiency (eff_n)	Proportion of Subsurface Flow (proportion_subsurface_n)	Retention Length (crit_len_n) (m)
1	Agriculture	12.0	0.25	0.30	200
2	Urban	16.4	0.05	0.05	200
3	Bare soil	9.0	0.00	0.05	200
4	Forest	0.9	0.80	0.60	200
5	Water	0.0	0.00	0.00	200
6	Pasture	5.5	0.35	0.40	200
7	Secondary vegetation	2.5	0.70	0.50	200
8	Oil palm	25.0	0.55	0.50	200
9	Other plantations	4.0	0.60	0.40	200
10	Cocoa	15.0	0.60	0.40	200

309

310

311

312 **Table S4.** The area of direct deforestation caused by cocoa cultivation in each district of UALL (measured in
 313 hectares).

Year/ District	Alexander von Humboldt	Irazola	Neshuya	Padre Abad	Curimana	Nueva Requena	Campoverde	Yarinacocha	Manantay	Total
2000	46	93	109	0	99	13	64	4	1	429
2001	54	39	100	0	77	10	93	14	2	389
2002	74	206	165	6	114	0	22	8	1	597
2003	20	87	118	5	31	2	71	9	0	344
2004	56	120	177	12	0	22	174	28	3	591
2005	9	2	15	9	0	0	116	7	0	158
2006	98	320	261	210	142	0	109	10	1	1151
2007	46	117	128	49	106	0	182	23	4	655
2008	71	283	185	107	251	0	132	8	1	1038
2009	47	306	138	155	284	1	96	9	1	1037
2010	51	168	60	65	126	0	96	5	8	579
2011	21	157	63	120	154	0	125	4	8	652
2012	59	412	153	234	402	42	135	2	5	1445
2013	54	376	94	112	208	33	113	2	0	992
2014	106	504	179	161	263	71	144	7	1	1436
2015	71	389	135	151	161	100	114	10	1	1134
2016	51	503	142	191	322	97	109	7	2	1424
2017	28	96	42	97	78	74	40	6	0	462
2018	53	434	90	207	304	234	51	7	0	1379
2019	61	264	108	183	338	378	220	8	0	1560

314

315 **Table S5.** The area and rate of deforestation from 2000 to 2020 in each district (measured in hectares).

District	Deforested Area (hectares)	Percentage of Total (%)	Forest Area in 2000 (hectares)	Deforestation Rate (%)
Irazola	4876	28	168678	2.89
Curimana	3463	20	176499	1.96
Neshuya	2463	14	41433	5.94
Campoverde	2206	13	63594	3.47
Padre Abad	2073	12	433763	0.48
Nueva Requena	1078	6	181790	0.59
Alexander von Humboldt	1075	6	9335	11.52
Yarinacocha	177	1	23210	0.76
Manantay	40	0	28769	0.14

316

317 **References**

- 318 Aybar, C., Fernández, C., Huerta, A., Lavado, W., Vega, F., Felipe-Obando, O., 2019.
319 Construction of a high-resolution gridded rainfall dataset for Peru from 1981 to the
320 present day. *Hydrological Sciences Journal* 65, 770–785.
321 <https://doi.org/10.1080/02626667.2019.1649411>
- 322 Castro, A., Dávila, C., Laura, W., Cubas Saucedo, F., Ávalos, G., López, C., Villena, D., Valdez,
323 M., Urbiola, J., Trebejo, I., Menis, L., Marín, D., 2021. Climas del Perú: mapa de
324 clasificación climática nacional, in: *Climas del Perú: mapa de clasificación climática*
325 nacional. pp. 70–70.
- 326 Charry, A., Torres, N., Fonseca, C., Narjes, M., 2023. The cocoa value chain in Ucayali: Analysis
327 to identify business models with agroecological potential.
- 328 Goñas, M., Rubio, K.B., Briceño, N.B.R., Pariente-Mondragón, E., Oliva-Cruz, M., 2022. Tree
329 diversity in agroforestry systems of native fine-aroma cacao, Amazonas, Peru. *PLOS*
330 *ONE* 17, e0275994. <https://doi.org/10.1371/journal.pone.0275994>
- 331 J, R., C., Alberdi, I., Bahamondez, C., Freitas, 2022. National Forest Inventories of Latin
332 America and the Caribbean: Towards the harmonization of forest information. Food &
333 Agriculture Org.
- 334 Lehner, B., 2014. HydroBASINS: Global watershed boundaries and sub-basin delineations
335 derived from HydroSHEDS.
- 336 NASA Jet Propulsion Laboratory, NASA, 2013. NASA Shuttle Radar Topography Mission Global
337 1 arc second (SRTMGL1) v003.
338 <https://doi.org/10.5067/MEASURES/SRTM/SRTMGL1.003>
- 339 Natural Capital Project, 2024. NDR: Nutrient Delivery Ratio — InVEST User Guide [WWW
340 Document]. URL
341 [https://storage.googleapis.com/releases.naturalcapitalproject.org/invest-](https://storage.googleapis.com/releases.naturalcapitalproject.org/invest-userguide/latest/en/ndr.html)
342 [userguide/latest/en/ndr.html](https://storage.googleapis.com/releases.naturalcapitalproject.org/invest-userguide/latest/en/ndr.html)
- 343 Pareja, P., Arce, A., Sánchez Choy, J.G., Velasquez, J.S., 2023. Context document (Peru):
344 Analysis of the context and agroecological principles in Ucayali's ALL.
- 345 Rajab, Y.A., Leuschner, C., Barus, H., Tjoa, A., Hertel, D., 2016. Cacao Cultivation under Diverse
346 Shade Tree Cover Allows High Carbon Storage and Sequestration without Yield Losses.
347 *PLOS ONE* 11, e0149949. <https://doi.org/10.1371/journal.pone.0149949>
- 348 Resolución Ministerial N.º 179-2021-MINAM [WWW Document], n.d. URL
349 <https://www.gob.pe/institucion/minam/normas-legales/2188100-179-2021-minam>
350 (accessed 7.17.25).
- 351 Rojas-Briceño, N.B., García, L., Cotrina-Sánchez, A., Goñas, M., Salas López, R., Silva López, J.O.,
352 Oliva-Cruz, M., 2022. Land Suitability for Cocoa Cultivation in Peru: AHP and MaxEnt
353 Modeling in a GIS Environment. *Agronomy* 12, 2930.
354 <https://doi.org/10.3390/agronomy12122930>
- 355 Silvestre, S.N.F. y de F., 2020. Inventario Nacional Forestal y de Fauna Silvestre, Informe de
356 resultados Panel 1. Servicio Nacional Forestal y de Fauna Silvestre.
357
358